Heliyon 10 (2024) e33502

Contents lists available at ScienceDirect

Heliyon

journal homepage: www.cell.com/heliyon

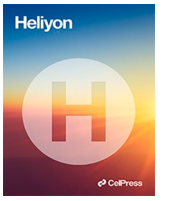

Research article

Derivation of novel metabolic pathway score identifies alanine metabolism as a targetable influencer of TNF-alpha signaling

Brandon N. D'Souza [a], Manoj Yadav [a], Prem Prashant Chaudhary [a], Grace Ratley [a], Max Yang Lu [a], Derron A. Alves [b], Ian A. Myles [a,*]

[a] *Labratory of Clinical Immunology and Microbiology, Epithelial Therapeutics Unit, National Institute of Allergy and Infectious Diseases, National Institutes of Health, Bethesda, MD, USA*

[b] *Infectious Disease Pathogenesis Section (IDPS), National Institute of Allergy and Infectious Diseases, National Institutes of Health, Bethesda, MD, USA*

A B S T R A C T

Background: Better understanding of the interaction between metabolism and immune response will be key to understanding physiology and disease. Tumor Necrosis Factor-alpha (TNFα) has been studied widely. However, despite the extensive knowledge about TNFα, the cytokine appears to induce not only variable, but often contradictory, effects on inflammation and cell proliferation. Despite advancements in the metabolomics field, it is still difficult to analyze the types of multi-dose, multi-time point studies needed for elucidating the varied immunologic responses induced by TNFα.

Results: We studied the dose and time course effects of TNFα on murine fibroblast cultures and further elucidated these connections using selective blockade of the TNF receptors (TNFR1 and TNFR2). To streamline analysis, we developed a method to collate the metabolic pathway output from MetaboAnalyst into a single value for the Index of pathway significance (IPS). Using this metric, we tested dose-, time-, and receptor-dependent effects of TNFα signaling on cell metabolism. Guided by these results, we then demonstrate that alanine supplementation enriched TNFR1-related responses in both cell and mouse models.

Conclusions: Our results suggest that TNFα, particularly when signaling through TNFR1, may preferentially use alanine metabolism for energy. These results are limited in by cell type used and immune outputs measured. However, we anticipate that our novel method may assist other researchers in identifying metabolic targets that influence their disease or model of interest through simplifying the analysis of multi-condition experiments. Furthermore, our results endorse the consideration of follow up studies in immunometabolism to improve outcomes in TNF-mediated diseases.

1. Introduction

The understanding of the mechanistic connection between metabolism and immune function continues to expand in modern research. One prominent example is the metabolic reprogramming that underlies innate cellular immune memory [1]. Additionally, a recent report demonstrates that interferon gamma (IFNg) signaling requires the nicotinamide phosphoribosyl transferase-nicotinamide adenine dinucleotide phosphate (NAMPT-NADPH) pathway to activate macrophages in culture [2]. The capacity for metabolomic analysis in immunology has greatly expanded via advances in mass spectrometry including improved proteomics, integration of RNAseq with metabolism, and spatial metabolomics [3–5]. Furthermore, programs, such as MetaboAnalyst, take large data sets on individual metabolisms and allow researchers to organize them into more manageable metabolic pathways [6]. However, evaluation of cytokine responses in immunology often requires experimental consideration of dosage, time course, and co-stimulatory factors. Each of these generate the need for multiple conditions. Despite how well metabolomic analyses can handle

* Corresponding author.
E-mail address: mylesi@niaid.nih.gov (I.A. Myles).

https://doi.org/10.1016/j.heliyon.2024.e33502
Received 21 December 2023; Received in revised form 21 June 2024; Accepted 21 June 2024
Available online 22 June 2024

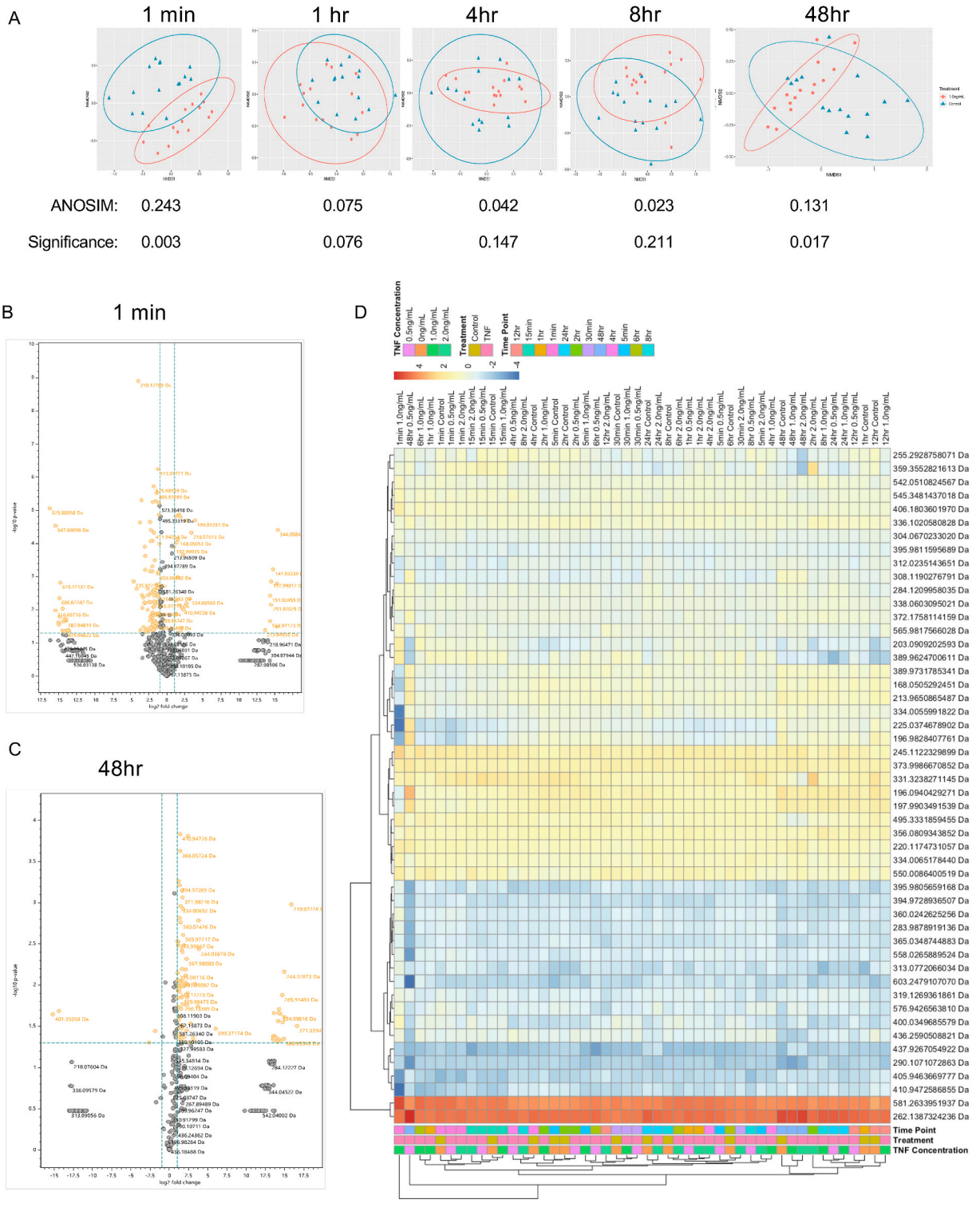

Fig. 1. Metabolic impact of TNFα stimulation in mouse fibroblasts. (A) Murine fibroblasts were stimulated with recombinant TNFα at 1 ng/mL. Supernatants were collected at indicated times and assessed for global differences by NMDS. (B–C) Volcano plots for 1-min (B) and 48-h (C) indicating differentially abundant metabolites between diluent (left) and TNFα stimulated (right) cells. (D) Top differentiating *m/z* values for indicated time and dose-response conditions for TNFα stimulation. Results represent three or more independent experiments.

large numbers of analytes, the analytic approaches are often limited in the number of experimental conditions they can compare. In this report we aimed to achieve two goals: (1) To develop a method to collate the available metabolic pathway data into a single value; and (2) assess actionable metabolic differences in the cellular response to tumor necrosis factor alpha (TNFα) using this method.

TNFα can mediate seemingly opposing responses of inflammation and immunity because of its ability to operate through two different receptors, TNF receptor 1 (TNFR1) and TNFR2. TNFR1 is associated with inflammation and apoptosis [7] while TNFR2 aids in cell activation, migration, and proliferation [8]. However, the standard characterization of TNFR1 as pro-inflammatory and TNFR2 as immune-modularly can vary by disease model [9,10]. Although of great clinical utility, because all current TNFα-blocking agents preclude the signaling pathways by binding to the TNF ligand through either receptor [9], current therapies leave many unanswered questions about optimizing clinical responses through differential impacts on the TNF receptors. Given that several papers have described the metabolic effects of TNFα on other organ systems [11–14], we hypothesized that the given metabolic conditions of immune cells may contribute to differential signaling between the TNFα receptors.

Herein we describe that collating MetaboAnalyst output data into a single value for the Index of Pathway Significance (IPS) suggests that dose and time dependent effects of TNFα signaling are heavily influenced by alanine metabolism. We further demonstrate that alanine supplementation alters TNF response in both cell and mouse models.

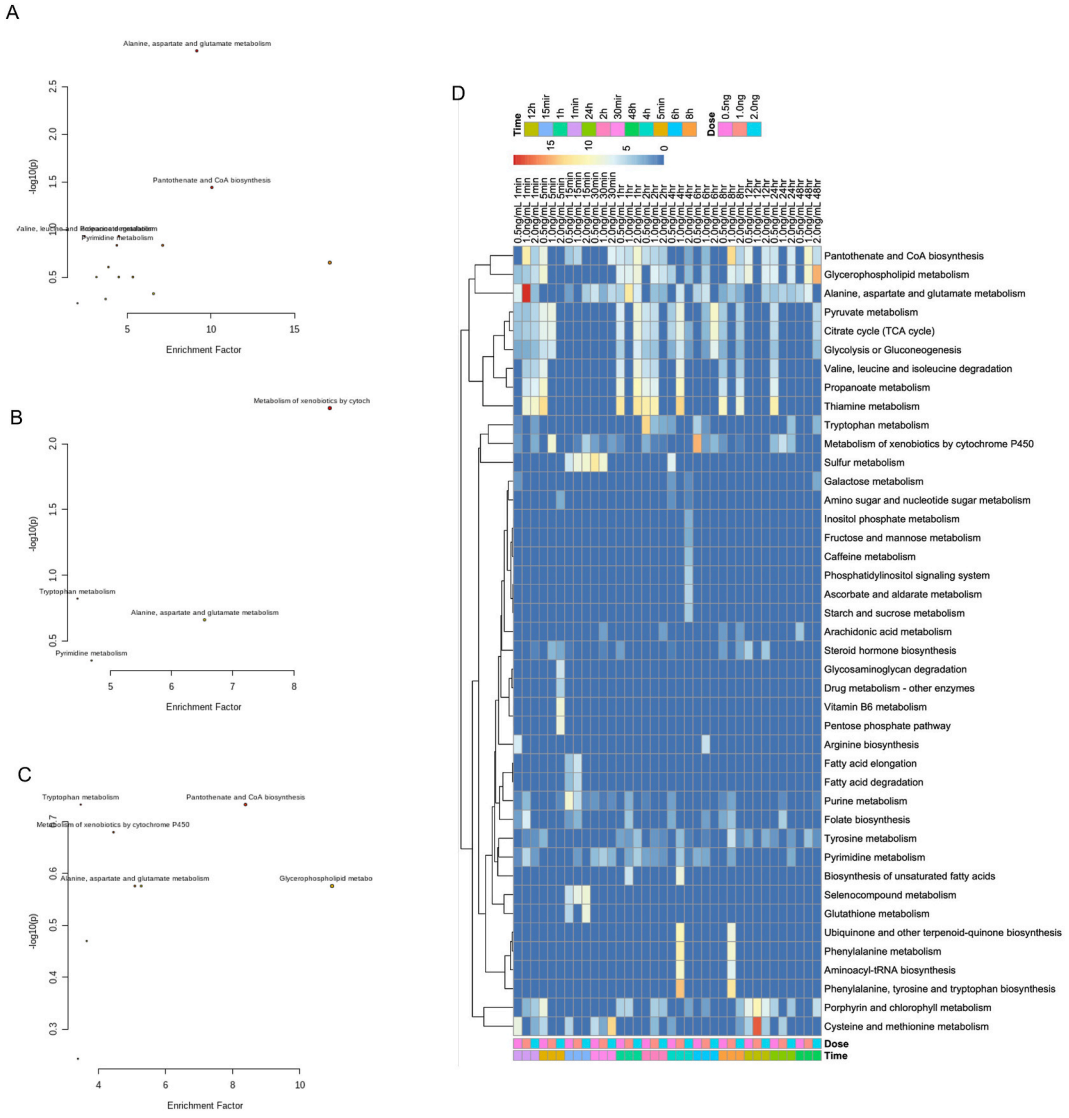

Fig. 2. Pathway analysis of TNFα stimulated fibroblasts implicates alanine metabolism. (A–C) MetaboAnalyst pathway output for 1 ng/mL TNFα for 1 min (A), 0.5 ng/mL at 6 h (B), and 2 ng/mL at 24 h. (D) Summarized IPS values derived from MetaboAnalyst pathway output for all indicated doses and timepoints. Results represent three or more independent experiments.

2. Results

2.1. TNFα exposure generates select differences in fibroblast metabolism

Metabolic profiles of TNF-treated 3T3 fibroblasts were compared to those of untreated cells. At each of the 12 time points, the supernatant from each well, along with cell lysates, were collected for metabolomic analysis. The overall similarity could be assessed by non-metric multidimensional scaling (NMDS) plots (Fig. 1a, Supplemental Fig. 1). NMDS is a multivariate statistical technique used

Fig. 3. IPS values allow for multi-condition comparisons. (A–C) IPS values for matrix of time and dose differences in TNFα stimulated fibroblasts for alanine metabolism (A), glycerophospholipids (B), and arginine metabolism (C). (D) IPS values for fibroblasts stimulated with 1 ng/mL of either TNFα or IL-1β. (E) IPS values super imposed onto KEGG metabolic pathway summary. Results represent three or more independent experiments.

for exploring and visualizing similarities or dissimilarities between objects or samples in a dataset. Unadjusted significance indicates differences in global metabolism at the 1-min, 1-h, and 48-h timepoints; however, adjusted values suggests no global differences arise with TNFα treatment of the cells. However, the intensity values for numerous individual peaks are significantly different at several timepoints (Fig. 1b–c, Supplemental Fig. 2). No single metabolite is significant across all conditions.

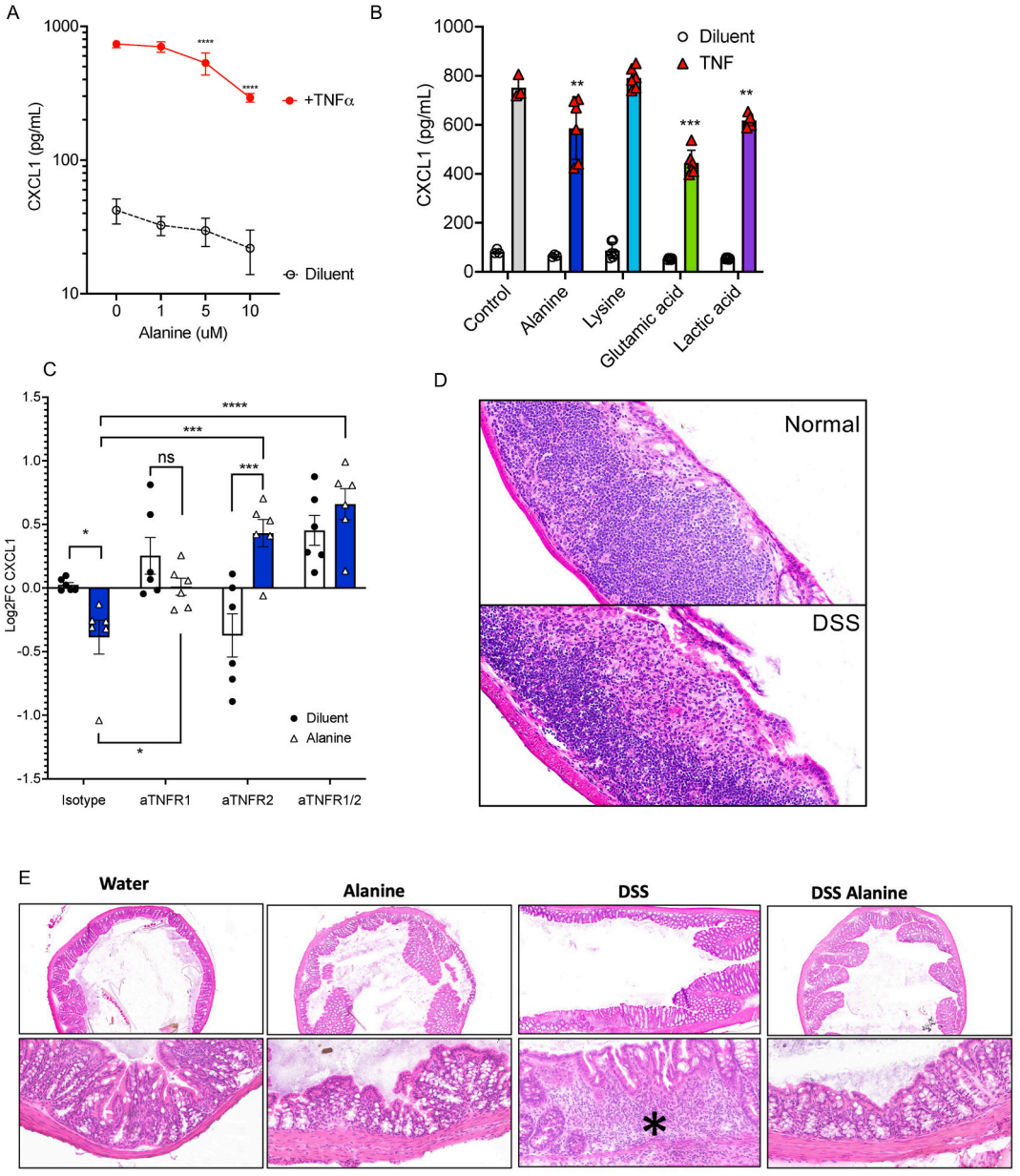

Fig. 4. Alanine exposure modulates models of TNF-induced immunity. (A) CXCL1 supernatant concentrations for mouse fibroblasts stimulated with TNFα (1 ng/mL) and indicated concentrations of alanine. (B) CXCL1 supernatant concentrations for mouse fibroblasts stimulated with TNFα (1 ng/mL) and 5 μM doses of indicated substance. (C) Log2 fold change (FC) for CXCL1 supernatant concentrations for mouse fibroblasts stimulated with TNFα (1 ng/mL), 5 μM alanine, with either isotype control or antibody blockade for TNF receptor 1 (TNFR1) and/or TFNR2. (D–E) Mice (N = 5 mice per group) were given water supplemented with 5 μM alanine, 5 % DSS, or 5 μM alanine + DSS. Colons were collected after 10–14 days of exposure and assessed for histologic evidence of inflammation. Images in D compare normal colonic gut associated lymphoid tissue (GALT) to the neutrophilic inflammation with mucosal ulceration in the GALT of a DSS mouse. In D, the segmental acute inflammation (*) in the lamina widely separating crypts (i.e. colitis) in the DSS-only mouse. Colons from mice given water, alanine, or DSS plus alanine are essentially normal. Results represent four (A–C) or two (D–E) independent experiments and are depicted as mean ± SEM. *: $p < 0.05$, **: $p < 0.01$, ***: $p < 0.001$; ****$p < 0.0001$; ns = not significant as determined by Student T test (A) or ANOVA (B–C).

2.2. Collating MetaboAnalyst output into a single value enhances multi-condition comparisons

MetaboAnalyst collates individual peak identifications into metabolic pathways defined by databases such as the Kyoto Encyclopedia of Genes and Genomes (KEGG). Although the visual (Fig. 2a, Supplemental Fig. 3) and numerical outputs reveal the metabolic pathways that demonstrate pathways with the greatest differences between two treatment conditions (Supplemental Fig. 3).

To address some of the limitations in pathway visualization, we developed a novel formula, the Index of Pathway Significance (IPS; see methods for details on derivation) that assigns a single, easily compared value to each pathway. IPS values are compared to each of the three TNF-treated conditions with the control group at each of the respective time points. This reveals that the largest differences are in alanine, aspartate, and glutamate metabolism (Fig. 2b). Use of IPS also facilitates comparisons within time points across various doses of TNFα stimulation (Fig. 3a–c) to establish pathways with consistent signatures rather than those with likely spurious values (Fig. 3c). Furthermore, interleukin (IL)-1β-treated fibroblasts demonstrate that the metabolic signature of TNFα activation is not shared with IL1β stimulated cells (Fig. 3d). The IPS values can also be superimposed upon the KEGG summary pathways to show the intensity that each pathway is altered by TNFα exposure (Fig. 3e; Supplemental Fig. 4).

2.3. Alanine impact on CXCL1 is TNFR1 dependent

Alanine was supplemented into cell media to investigate the effects of TNFα under alanine-enriched conditions. CXCL1 is a chemoattractant for immune cells, including neutrophils, and its release is stimulated by TNFα [15]. Because of its known involvement in cell migration [16], as well as inflammation [17], this chemokine was used as a representative measurement of functioning immune response. C-X-C motif ligand 1 (CXCL1) concentrations are higher in the supernatant of cells challenged with TNFα; alanine supplementation results in significantly less CXCL1 release compared to diluent in a dose dependent manner (Fig. 4a). Neither lysine, glutamic acid, nor lactic acid significantly impact CXCL1 production in TNF-naïve cells (Fig. 4b). However, glutamic and lactic acid inhibit CXCL1 from TNF-treated fibroblasts (Fig. 4b), suggesting a partial role for pH in the effects of alanine.

As before, when both TNF receptors are available, alanine inhibits CXCL1 production. However, the significance of this effect is ablated by blockade of TNFR1 (Fig. 4c). While alanine continues to alter CXCL1 production under blockade of TNRFR2, the impact appears paradoxical (Fig. 4c). Effects are not significant when the cells are challenged with either glutamic acid or lysine (Supplemental Figs. 5a–b). Supplementation with lactic acid significantly enhances CXCL1 release when TNFR1 is blocked (Supplemental Fig. 5c).

2.4. Alanine supplementation normalizes outcomes in DSS colitis

Given prior reports of the TNFR1 dependance of the murine DSS colitis model [10], we supplemented DSS drinking water with 5 nM alanine. 40 % of mice in the DSS treated group demonstrate either focal extensive neutrophilic inflammation effacing the gut associated lymphoid tissue (GALT) or segmental neutrophilic infiltration in the lamina propria that separates and replaces crypts and extends into the submucosa (Fig. 4d–e). However, these effects were ablated by alanine supplementation (Fig. 4d). Alanine treatment alone did not impact weight change or histology.

3. Discussion

Analysis tools such as those provided by MetaboAnalyst have greatly improved metabolomic workflows by summarizing complex data sets of individual metabolites into pathways that may be experimentally investigated for therapeutic potential. In this work, we sought to expand on the ability to perform pathway analysis across numerous conditions of dose, time, and cofactor exposure. To our knowledge, the effects of TNFα on metabolism have not been thoroughly studied at the cellular level in immune cells, despite descriptions of metabolic impacts in non-immunologic tissue [11–14].

TNFα is a cytokine primarily produced by activated macrophages or T lymphocytes [7], but also expressed by a variety of other cell lines [18]. When existing as a transmembrane protein, it has a molecular mass of 26 kDa, however, can be secreted as a 17 kDa protein under certain conditions with the help of TNF-alpha-activating converting enzyme (TACE) [19]. While TNFα levels are typically undetectable in healthy individuals [7], abnormal concentrations in the serum, tissue, or stool are associated with a wide array of diseases, including asthma [20], HIV [21], Crohn's disease [22], diabetes [23], and psoriasis [24], among others. Furthermore, serum levels frequently correlate with the severity of the disease [25].

Our investigation identifies alanine, aspartate, and glutamate metabolism as being the most significantly different pathway between TNF-treated fibroblasts. Supplementation with alanine alters the CXCL1 production of these cells in a TNFR-sensitive manner and could be used to improve outcomes in the TNFR-dependent model of DSS colitis [10]. This finding provides additional detail about the underlying cellular activity that goes beyond the heavily studied bioactivities associated with each of the two TNF receptors.

Along with differences in structure and signaling pathways [26,27], TNFR1 and TNFR2 can differ with respect to percentage of cells expressing each type of receptor, as well as the number of receptors per cell. For example, when looking specifically at peripheral immune cells, both measurements have been found to be higher for TNFR2 compared to TNFR1 [28]. That said, while TNFR1 is nearly omnipresent [29], TNFR2 is limited to certain cell types, including myeloid cells, regulatory T-cells, glial cells, and some endothelial cells, along with being induced in epithelial cells and fibroblasts [30]. TNFR1 and TNFR2 differ further when discussing the TNFα molecules that they can bind and their preferences for each. While transmembrane TNFα (tmTNFα) can efficiently activate TNFR1 and TNFR2 signaling pathways, soluble TNF (sTNFα) only activates TNFR1 to a high degree [31]. This is due to sTNFα's low attraction to

TNFR2, and the dissociation that is still possible after initial binding [32].

Our work suggest that the metabolic state of fibroblasts may exert additional influence over TNFα signaling in general as well as specific responses to the differential signaling through the TNF receptors. In the light of the literature indicating that TNFR1 ablation worsens outcomes in DSS colitis [10], our cell and mouse model results suggest that alanine supplementation preferentially enhances signaling through TNFR1 and suggests opposing impacts on CXCL1 by TNFR1 and TNFR2. Furthermore, the results indicating that alanine's impact on CXCL1 is TNFR1-dependent suggest a bi-directional crosstalk between immunity and metabolism. Alanine's role in the alanine-cycle may lend to future experiments using inhibitors of glutamic-pyruvic transaminase (GPT) to assess their impact on TNFα signaling. In addition, in vitro systems capable of discerning TNFR1 versus TNFR2 activation in real time would greatly aid the field.

However, our work is limited in several ways. First, our findings are restricted to fibroblast cultures and murine models of general TNF response. These findings would greatly benefit from mouse model validation in additional disease models that are known to be influenced by TNF such as tuberculosis or rheumatic ailments [9] as well as challenging other cell types that are TNFα modulated. Second, we limited our functional output to CXCL1 production for simplicity, but the potential effects of TNFα go far beyond this single chemokine. Third, while alanine supplementation had differing impacts than glutamic acid or lactic acid, the possible contribution of pH cannot be excluded; however, separating the impacts of select amino acids without chemically altering them via buffers is not likely to be a viable approach. Finally, while our IPS formula was derived systematically and validated previously [33], alternative equations could lead to different results. However, while we cannot present this work as a definitive analysis of the metabolic impact of TNFα, we were able to use our novel metabolic pathway metric to identified alanine as a modulator of TNFα response in both cell and mouse models.

Overall, our results offer a novel addition to current metabolomic workflows that may allow researchers to assess large numbers of conditions more readily for metabolic pathways with the potential for therapeutic manipulation. Ultimately, we hope that the integration of the IPS into metabolic workflows may further enhance the identification of targetable metabolic pathways that may improve immunologic outcomes.

4. Materials and methods

4.1. Cell culture

NIH/3T3 Mouse Fibroblasts were previously purchased from ATCC. A frozen cryovial was thawed and cultured in DMEM (gibco; #11965092) containing 10 % FBS and 100 μg/mL penicillin/streptomycin glutamine (gibco; #15140122). After nearing full confluence in a T75 flask, cells were trypsinized with 0.05 % trypsin-EDTA (gibco; #25300054) and seeded on 24 well plates (corning; #3524) at 70,000 cells per well concentration, one for each time point of interest. Plates were then incubated for a minimum of 24 h, or until 75 % confluence was achieved, and each treatment condition was plated in triplicates. After 24 h, cells were treated with different conditions and cell supernatant, as well as cell lysates, were collected and stored at −80 °C until further use.

Cells were exposed to any added organic compounds and/or antibodies 6 h before start of the experiment (t = −6), and 550 μL of fresh DMEM media containing the same supplements, as well as TNFα (#300-01A) from Peprotech when appropriate, was added at t = 0 at 0.5 ng/mL to 2 ng/mL as indicated. Plates were then returned to the incubator until their specific time point.

4.2. In vitro sample collection

At each time point, the specific plate was taken from the incubator and cell supernatant was transferred from each well to a different Eppendorf tube. In the initial exploratory trial, 250 μL of pure methanol at room temperature was then added to each well for cell lysis. This volume was later adjusted to 500 μL. Cells remained in the methanol for 20 min, and occasional mechanical irritation of the plate was used to promote the rupturing. Once complete, the contents of each well were removed and added to the same Eppendorf tube as the supernatant in the case of the exploratory trial, and different tubes in subsequent trials. All tubes were then frozen at −80° Fahrenheit.

4.3. Mass spectrometry

To assist in mass spectrometry data collection, a matrix consisting of 90 % MeOH, 20 mg/mL 2,5-dihydroxybenzoic acid matrix (Sigma Aldrich; 85,707), and 0.01 % TFA (Sigma; T6508) was prepared. Collected samples were thawed and a 3:2:1 ratio of matrix: supernatant:lysate was prepared for each individual sample. 2 μL from each prepared solution was spotted onto a metal spot plate and run through MALDI timsTOF Fleximager (Bruker Daltonik, Bremen, Germany). Specifically, the machine was operating in TIMS qTOF positive ion mode from m/z 200 to 2000 with a laser intensity of 75 %. Additional settings were as previously described [5].

4.4. Index of Pathway Significance

The Index of Pathway Significance (IPS) is an in-house formula derived from five metrics provided by MetaboAnalyst: total number of metabolites in a metabolic pathway, the total number of metabolite hits picked up from a sample, the number of significant metabolite hits in a pathway, the expected number of total metabolite hits in a sample, and FET, the p-value associated with a sample. When considered together, they produce a single, easily comparable value that is associated with differences between two treatments

with respect to a certain metabolic pathway. A higher IPS values indicates a greater difference and can be used to rank either the metabolic pathways that are shared between two treatments, or the treatments that all exhibit that particular pathway. Assigning a single value to each pathway also allows many comparisons to be condensed and visualized in figures such as heat maps and metabolic pathway maps.

In the formula, the placement of each of the five metrics was logically determined based on how its manipulation would affect the final IPS value. The numerator consists of the weighted sum of significant and non-significant metabolites that were found in the samples of interest and divides it by the total number of metabolites in that same pathway. While all metabolites that were found to be different between the samples of interest are important, those whose differences were statistically significant were deemed more so, and consequently, the number of significant metabolites was squared. The total number of metabolites in a given pathway was placed in the denominator of the ratio, as the number of identified metabolites is expected to increase as the number of identifiable metabolites increases. In other words, with all other metrics being equal, identifying five metabolites in a pathway with ten total metabolites is more significant than identifying five metabolites in a pathway with fifty total metabolites. This ratio is then divided by the number of metabolites from that pathway that MetaboAnalyst expected to find in the samples, with a lower value further underscoring the significance of any and all identified metabolites. With FET, or p-value, being perhaps the metric most indicative of differences between two samples, it is squared and positioned in the denominator to increase the final IPS score exponentially as it approaches or passes statistical significance. Finally, to avoid calculating the same IPS value when the number of significant metabolites is zero and one, respectively, one is added to the final quotient.

To validate the placement of each of the five metrics, as well as the degree to which they affected the final IPS value, arbitrary data was created, and each metric was manipulated individually.

4.5. Cytokine assay

After experiments, cultured cell supernatant was stored at −80 °C before being used to measure cytokine level. We have used the Bio-Plex Pro mouse Th17 cytokine assay kit from Bio-Rad (12010828) and protocol was followed according to manufacturer instructions. 50 μl of diluted beads were added to each well of the assay plate. Followed by washing the plate with 100 μl of Bio-Plex wash buffer. 50 μl of samples, standard, and a blank were added to respective wells. The plate was then incubated in the dark for 1 h at room temperature with vigorous shaking before being washed 3 times with a wash buffer and the addition of 25 μl of detection antibodies in each well. This was followed by incubating the plate in the dark for 30 min with vigorous shaking, and the plate was washed 3 times with a wash buffer. Then, 50 μl 1× straptavidin-PE (SA-PE) was added in each well before the plate was incubated in the dark for 10 min with vigorous shaking. Finally, we washed the plate three times with 100 μl wash buffer, resuspend beads in 125 μl assay buffer, covered it, and placed it in the shaker at 850 rpm for 30 s. Reading samples were taken with the Bio-Plex 200 system from Bio-Rad.

4.6. Mice

All mice were purchased from the Jackson laboratory. C57BL/6 mice aged 6–10 weeks were used for experiments with age and sex matched within each experiments. 5 % DSS (Sigma) was dissolved into the mouse drinking water. Mice (N = 5 per group) were allowed to drink ad libitum for 10–14 days prior to collection of histology tissue. Tissues were mounted and stained with H&E by Histoserv Inc (Germantown, MD). Colon sections were examined by light microscopy using an Olympus BX51 microscope and photomicrographs were taken using an Olympus DP28 camera. Mice experiments were performed under the approval and supervision of the NIAID Animal Care Protocols.

4.7. Statistics

All MALDI imaging data were visualized using SciLS Lab Version 2021 (Bruker Daltonics). Statistical analyses were conducted in R, including hierarchical clustering. Intensity data was pareto scaled and log transformed. ANOVA was used to identify group differences when >2 groups were compared, Student T test was used when only 2 groups were compared. P-values were adjusted using the Benjamini and Hochberg method.

Ethics statement

This study was reviewed and approved by the Animal Study Protocol committee of the National Institute of Allergy and Infectious Diseases, with the approval number LCIM8E.

Data availability

All data are included in the article of supplemental materials. Raw metabolomics files can be shared upon reasonable request.

CRediT authorship contribution statement

Brandon N. D'Souza: Writing – review & editing, Writing – original draft, Visualization, Validation, Project administration, Methodology, Investigation, Formal analysis, Data curation. **Manoj Yadav:** Writing – review & editing, Writing – original draft,

Visualization, Validation, Supervision, Project administration, Methodology, Investigation, Formal analysis, Data curation. **Prem Prashant Chaudhary:** Writing – review & editing, Visualization, Validation, Supervision, Software, Methodology, Investigation, Formal analysis. **Grace Ratley:** Writing – review & editing, Visualization, Validation, Methodology. **Max Yang Lu:** Writing – review & editing, Visualization, Validation, Investigation, Data curation. **Derron A. Alves:** Writing – review & editing, Visualization, Validation, Supervision, Software, Resources, Project administration, Methodology, Investigation, Funding acquisition, Formal analysis. **Ian A. Myles:** Writing – review & editing, Writing – original draft, Visualization, Validation, Supervision, Software, Resources, Project administration, Methodology, Investigation, Funding acquisition, Formal analysis, Data curation.

Declaration of competing interest

The authors declare that they have no known competing financial interests or personal relationships that could have appeared to influence the work reported in this paper.

Acknowledgements

This work was supported by the Division of Intramural Research Program of the National Institute of Allergy and Infectious Diseases (NIAID) and the National Institutes of Health (NIH). We would like to give special thanks to Mahnaz Minai, Kevin Bock, and Bianca Nagata in NIAID's Infectious Disease Pathogenesis Section (IDPS) for their pathology technical expertise.

Appendix A. Supplementary data

Supplementary data to this article can be found online at https://doi.org/10.1016/j.heliyon.2024.e33502.

References

[1] J. Dominguez-Andres, L.A. Joosten, M.G. Netea, Induction of innate immune memory: the role of cellular metabolism, Curr. Opin. Immunol. 56 (2019) 10–16.
[2] K.J. McCann, S.M. Christensen, D.H. Colby, P.J. McGuire, I.A. Myles, C.S. Zerbe, C.L. Dalgard, G. Sukumar, W.J. Leonard, B.A. McCormick, et al., IFNgamma regulates NAD+ metabolism to promote the respiratory burst in human monocytes, Blood Adv 6 (12) (2022) 3821–3834.
[3] A. Halder, A. Verma, D. Biswas, S. Srivastava, Recent advances in mass-spectrometry based proteomics software, tools and databases, Drug Discov. Today Technol. 39 (2021) 69–79.
[4] Y. Su, D. Yuan, D.G. Chen, R.H. Ng, K. Wang, J. Choi, S. Li, S. Hong, R. Zhang, J. Xie, et al., Multiple early factors anticipate post-acute COVID-19 sequelae, Cell 185 (5) (2022) 881–895 e820.
[5] M. Yadav, P.P. Chaudhary, B.N. D'Souza, J. Spathies, I.A. Myles, Impact of skin tissue collection method on downstream MALDI-imaging, Metabolites 12 (6) (2022).
[6] Z. Pang, J. Chong, G. Zhou, D.A. de Lima Morais, L. Chang, M. Barrette, C. Gauthier, P.E. Jacques, S. Li, J. Xia, MetaboAnalyst 5.0: narrowing the gap between raw spectra and functional insights, Nucleic Acids Res. 49 (W1) (2021) W388–W396.
[7] J.R. Bradley, TNF-mediated inflammatory disease, J. Pathol. 214 (2) (2008) 149–160.
[8] E.H. Choy, G.S. Panayi, Cytokine pathways and joint inflammation in rheumatoid arthritis, N. Engl. J. Med. 344 (12) (2001) 907–916.
[9] P. Gough, I.A. Myles, Tumor necrosis factor receptors: pleiotropic signaling complexes and their differential effects, Front. Immunol. 11 (2020) 585880.
[10] K. Wang, G. Han, Y. Dou, Y. Wang, G. Liu, R. Wang, H. Xiao, X. Li, C. Hou, B. Shen, et al., Opposite role of tumor necrosis factor receptors in dextran sulfate sodium-induced colitis in mice, PLoS One 7 (12) (2012) e52924.
[11] X. Chen, K. Xun, L. Chen, Y. Wang, TNF-alpha, a potent lipid metabolism regulator, Cell Biochem. Funct. 27 (7) (2009) 407–416.
[12] B. Seriolo, S. Paolino, A. Sulli, V. Ferretti, M. Cutolo, Bone metabolism changes during anti-TNF-alpha therapy in patients with active rheumatoid arthritis, Ann. N. Y. Acad. Sci. 1069 (2006) 420–427.
[13] C. Popa, M.G. Netea, P.L. van Riel, J.W. van der Meer, A.F. Stalenhoef, The role of TNF-alpha in chronic inflammatory conditions, intermediary metabolism, and cardiovascular risk, J. Lipid Res. 48 (4) (2007) 751–762.
[14] A.H. Remels, H.R. Gosker, K.J. Verhees, R.C. Langen, A.M. Schols, TNF-alpha-induced NF-kappaB activation stimulates skeletal muscle glycolytic metabolism through activation of HIF-1alpha, Endocrinology 156 (5) (2015) 1770–1781.
[15] H.M. Lo, T.H. Lai, C.H. Li, W.B. Wu, TNF-alpha induces CXCL1 chemokine expression and release in human vascular endothelial cells in vitro via two distinct signaling pathways, Acta Pharmacol. Sin. 35 (3) (2014) 339–350.
[16] T.L. Yew, Y.T. Hung, H.Y. Li, H.W. Chen, L.L. Chen, K.S. Tsai, S.H. Chiou, K.C. Chao, T.F. Huang, H.L. Chen, et al., Enhancement of wound healing by human multipotent stromal cell conditioned medium: the paracrine factors and p38 MAPK activation, Cell Transplant. 20 (5) (2011) 693–706.
[17] P. Dhawan, A. Richmond, Role of CXCL1 in tumorigenesis of melanoma, J. Leukoc. Biol. 72 (1) (2002) 9–18.
[18] G. Sethi, B. Sung, B.B. Aggarwal, TNF: a master switch for inflammation to cancer, Front. Biosci. 13 (2008) 5094–5107.
[19] N. Watanabe, K. Nakada, Y. Kobayashi, Processing and release of tumor necrosis factor alpha, Eur. J. Biochem. 253 (3) (1998) 576–582.
[20] E. Noguchi, Y. Yokouchi, M. Shibasaki, M. Inudou, S. Nakahara, T. Nogami, M. Kamioka, K. Yamakawa-Kobayashi, K. Ichikawa, A. Matsui, et al., Association between TNFA polymorphism and the development of asthma in the Japanese population, Am. J. Respir. Crit. Care Med. 166 (1) (2002) 43–46.
[21] P. Aukrust, N.B. Liabakk, F. Muller, E. Lien, T. Espevik, S.S. Froland, Serum levels of tumor necrosis factor-alpha (TNF alpha) and soluble TNF receptors in human immunodeficiency virus type 1 infection–correlations to clinical, immunologic, and virologic parameters, J. Infect. Dis. 169 (2) (1994) 420–424.
[22] S.J. Van Deventer, Tumour necrosis factor and Crohn's disease, Gut 40 (4) (1997) 443–448.
[23] J.J. Swaroop, D. Rajarajeswari, J.N. Naidu, Association of TNF-alpha with insulin resistance in type 2 diabetes mellitus, Indian J. Med. Res. 135 (1) (2012) 127–130.
[24] E. Ogawa, Y. Sato, A. Minagawa, R. Okuyama, Pathogenesis of psoriasis and development of treatment, J. Dermatol. 45 (3) (2018) 264–272.
[25] R.G. Titus, B. Sherry, A. Cerami, The involvement of TNF, IL-1 and IL-6 in the immune response to protozoan parasites, Immunol. Today 12 (3) (1991) A13–A16.
[26] H. Wajant, D. Siegmund, TNFR1 and TNFR2 in the control of the life and death balance of macrophages, Front. Cell Dev. Biol. 7 (2019) 91.
[27] Y. Mukai, T. Nakamura, M. Yoshikawa, Y. Yoshioka, S. Tsunoda, S. Nakagawa, Y. Yamagata, Y. Tsutsumi, Solution of the structure of the TNF-TNFR2 complex, Sci. Signal. 3 (148) (2010) ra83.
[28] S.V. Sennikov, A.A. Alshevskaya, J. Zhukova, I. Belomestnova, A.V. Karaulov, J.A. Lopatnikova, Expression density of receptors as a potent regulator of cell function and property in Health and pathology, Int. Arch. Allergy Immunol. 178 (2) (2019) 182–191.

[29] J.M. Dopp, T.A. Sarafian, F.M. Spinella, M.A. Kahn, H. Shau, J. de Vellis, Expression of the p75 TNF receptor is linked to TNF-induced NFkappaB translocation and oxyradical neutralization in glial cells, Neurochem. Res. 27 (11) (2002) 1535–1542.
[30] J. Medler, H. Wajant, Tumor necrosis factor receptor-2 (TNFR2): an overview of an emerging drug target, Expert Opin. Ther. Targets 23 (4) (2019) 295–307.
[31] H. Wajant, K. Pfizenmaier, P. Scheurich, Tumor necrosis factor signaling, Cell Death Differ. 10 (1) (2003) 45–65.
[32] M. Grell, E. Douni, H. Wajant, M. Lohden, M. Clauss, B. Maxeiner, S. Georgopoulos, W. Lesslauer, G. Kollias, K. Pfizenmaier, et al., The transmembrane form of tumor necrosis factor is the prime activating ligand of the 80 kDa tumor necrosis factor receptor, Cell 83 (5) (1995) 793–802.
[33] M. Yadav, P.P. Chaudhary, B.N. D'Souza, G. Ratley, J. Spathies, S. Ganesan, J. Zeldin, I.A. Myles, Diisocyanates influence models of atopic dermatitis through direct activation of TRPA1, PLoS One 18 (3) (2023) e0282569.